JACS
JOURNAL OF THE AMERICAN CHEMICAL SOCIETY
Article
pubs.acs.org/JACS

The Presence of an Air−Water Interface Affects Formation and Elongation of α-Synuclein Fibrils

Silvia Campioni,[†] Guillaume Carret,[†,‡] Sophia Jordens,[§] Lucrèce Nicoud,[∥] Raffaele Mezzenga,[§] and Roland Riek*[,†]

[†]Laboratory of Physical Chemistry, Department of Chemistry and Applied Biosciences, Swiss Federal Institute of Technology Zurich, Wolfgang-Pauli-Str. 10, 8093 Zurich, Switzerland

[‡]Department of Chemistry, École Normale Supérieure, 24 rue Lhomond, 75005 Paris, France

[§]Institute of Food, Nutrition and Health, Department of Health Sciences and Technology, Swiss Federal Institute of Technology Zurich, Schmelzbergstrasse 9, 8092 Zurich, Switzerland

[∥]Institute for Chemical and Bioengineering, Department of Chemistry and Applied Biosciences, Swiss Federal Institute of Technology Zurich, Wolfgang-Pauli-Str. 10, 8093 Zurich, Switzerland

Supporting Information

ABSTRACT: The aggregation of human α-Synuclein (α-Syn) into amyloid fibrils is related to the onset of multiple diseases termed synucleinopathies. Substantial evidence suggests that hydrophobic−hydrophilic interfaces promote the aggregation of amyloidogenic proteins and peptides in vitro. In this work the effect of the air−water interface (AWI) on α-Syn aggregation is investigated by means of thioflavin T binding measurements, dynamic light scattering, size-exclusion chromatography, electron microscopy, and atomic force microscopy. Measurements were performed with the monomeric protein alone or together with preformed seeds. In presence of the AWI, α-Syn aggregates readily into amyloid fibrils that remain adsorbed to the AWI. Instead, when the AWI is removed from the samples by replacing it with a solid−liquid interface, the interfacial aggregation of monomeric α-Syn is greatly reduced and no significant increase in ThT fluorescence is detected in the bulk, even at 900 μM concentration. Bulk aggregation is observed only when a sufficient amount of preformed seeds is added, and the initial slope of the kinetics scales with the amount of seeds as expected for first order kinetics. By contrast, in seeded experiments with the AWI, the initial slope is one order of magnitude lower and secondary nucleation pathways appear instead to be dominant. Thus, interfaces play multiple roles in the aggregation of α-Syn, influencing primary nucleation, aggregate elongation, and secondary nucleation processes. Interfacial effects must therefore be taken into account to achieve a complete understanding of protein aggregation events in vitro as well as in vivo.

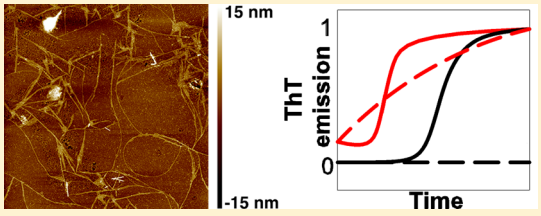

INTRODUCTION

The aggregation of soluble peptides and proteins into amyloid fibrils is the hallmark of more than 50 human disorders, including severe neurodegenerative pathologies.[1−3] Considerable effort was therefore spent in the last decades to elucidate the structure of the fibrils,[2] their mechanism of formation,[4,5] and the factors influencing such aggregation processes.[6] Amyloid fibrils are generally formed through nucleation-dependent polymerization, which is characterized by a lag-phase (attributed at the microscopic level to the energetically unfavorable nucleation step) followed by rapid growth and elongation of the nuclei, or seeds, into fibrils and a final stationary phase that reflects the equilibrium between fibrils and monomers.[5,7,8] Aggregation kinetics are often monitored by means of thioflavin T (ThT) binding measurements, a dye that specifically recognizes the cross-β structure typical of amyloid fibrils.[9,10] The factors so far considered to determine the aggregation behavior in vitro of proteins/peptides are mainly their intrinsic (sequence-based) propensity to aggregate,[6,11] the sample conditions (concentration, pH, presence of cosolvents, ionic strength),[12,13] and the incubation conditions (temperature, volume of sample, presence/absence of shaking).[14−16]

An additional but often neglected factor that influences aggregation kinetics measured in vitro is the presence of surfaces, and particularly of hydrophobic−hydrophilic interfaces (HHIs).[17] Many amyloidogenic proteins and peptides possess an amphiphilic character and surfactant-like properties: not only do they concentrate at HHIs, but they also adopt there an orientation and a conformation that favors fibril formation.[18−23] Recent studies on the islet amyloid polypeptide (IAPP) and the amyloid-β (Aβ) peptide, involved in type II diabetes mellitus and Alzheimer's disease, respectively, indicate that HHIs are critical for their aggregation to occur, especially at low concentration.[24−26] HHIs also trigger the self-assembly of class I fungal hydrophobins and a bacterial hydrophobin, whose aggregates are instead functional.[23,27]

Received: November 27, 2013
Published: January 24, 2014

   dx.doi.org/10.1021/ja412105t | J. Am. Chem. Soc. 2014, 136, 2866−2875

Human α-Synuclein (α-Syn) is the major component of the fibrillar deposits found in the brain of Parkinson's disease patients.[28,29] Its aggregation mechanism under conditions of pH and temperature close to physiological ones and in the absence of any aggregation-promoting additive has been proven difficult to establish, also due to the poor reproducibility of α-Syn aggregation kinetics measured in vitro.[16,30] To increase the extent of reproducibility of the kinetics without moving to nonphysiological conditions, α-Syn samples are in general aggregated under constant agitation, which, among other effects, also increases the area of the air−water interface (AWI), a type of HHI.[16,30] In sealed samples (without AWI) at fixed protein concentration and agitated with beads made of three different materials, α-Syn aggregated only in the presence of the most hydrophobic bead type, suggesting that the aggregation promoting effect given by a HHI dominates over other agitation-induced effects such as increased collision rates and enhanced fibril fragmentation.[31] However, compared to other types of HHIs, the AWI is ubiquitously present in in vitro experiments and its effects are usually not accounted for.

In this work, the role of the AWI on the aggregation kinetics of α-Syn at different protein concentrations or with increasing amounts of preformed seeds is investigated. Removal of such an interface inhibits the aggregation of the monomeric protein even at high protein concentration. In seeded experiments, the AWI accelerates aggregation at any seed concentration, even if nucleation is not fully bypassed. However, at high seed concentrations, aggregation can happen in the bulk too and at a faster rate than at the AWI. Finally, the fibrils formed in the presence of the AWI are found to be surface active and form a dense layer at the interface. Overall, these data contribute to the understanding of the factors that influence α-Syn aggregation in vitro and suggest that in vivo HHIs, such as those provided by biological membranes, may play a yet underestimated role in promoting not only the aggregation of the monomeric protein but also the growth of internalized α-Syn fibrils/seeds.[32]

RESULTS

AWI Removal Suppresses the Aggregation of Monomeric α-Syn at Different Protein Concentrations. With the experimental setup described in the Supporting Information the effect of AWI removal on aggregation kinetics with monomeric α-Syn was first tested (Supplementary Results and Figure S1). A sample containing 300 μM α-Syn and 20 μM ThT in phosphate buffered saline (PBS) with 0.05% sodium azide (NaN_3), pH 7.4, was dispensed into the various wells of a 96-well plate: some were immediately capped to remove the AWI; others were left with an air space above the dispensed volume. The final sample volume and the heights of the air−water and cap−water interfaces are similar. Figure 1A shows the results of multiple ThT binding kinetics performed at 37 °C. The plate was left quiescent except for a 5 s shaking time at 500 rpm every 20 min, just before each measurement. The data collected in the presence of the AWI correspond to the average curve and standard deviation (error bars) of the ThT emission data from 80 wells measured in 14 independent plates, each with a fresh protein preparation. Those without an AWI refer to 10 independent plates, for a total of 74 wells. The results indicate that, under these experimental conditions, ca. 4 days of incubation is needed to detect α-Syn aggregation when the AWI is present. Upon aggregation, the emission of ThT increases by a factor of ca. 500−600 with respect to control wells having the same amount of dye but no protein and, during incubation, the sample becomes partially gelatinous (data not shown). Instead, when the AWI is removed at the beginning of the experiment, a significant increase in ThT fluorescence over time is no longer observed on the same time-scale, and the maximum intensity of ThT fluorescence is more than two orders of magnitude smaller than that of corresponding samples with the AWI (Figure 1B).

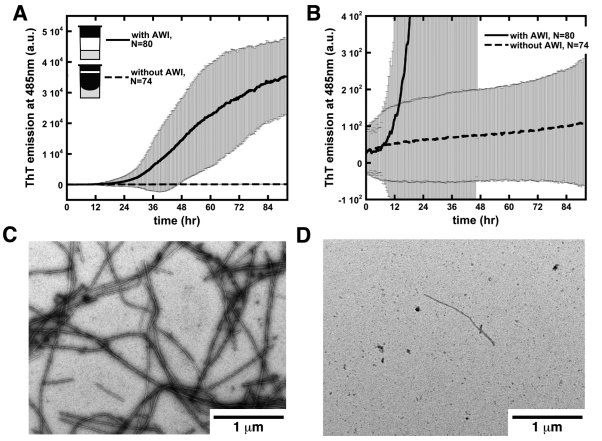

Figure 1. Effect of AWI removal on α-Syn aggregation at 300 μM concentration. (A, B) ThT emission curves from wells incubated with (solid line) and without (dashed line) the AWI. Error bars show the standard deviations of the two sets of data. Panel (A) shows also a schematic drawing of the setup used. A light gray area shows the sample volume. The transparent PMMA caps (black) and the O-ring (white) are shown in inverted colors to help visualization. A more detailed drawing is in the Supporting Information. (B) Zoom-in of the data shown in panel (A) to better show the results obtained without the AWI. (C, D) EM images of aliquots of samples recovered from the plate after incubation with (C) and without (D) the AWI.

To rule out that, in the absence of the AWI, aggregation into species that are not capable to bind the ThT dye occurred, the samples from wells incubated for 4 days either with or without the AWI were merged after collection, and an aliquot was used for electron microscopy (EM). The EM images of the samples incubated with the AWI show many 15−20 nm wide and several micrometers long fibrils (Figure 1C). By contrast, amyloid fibrils are rarely found in samples incubated without the AWI (Figure 1D). Rather, in this latter case, spherical and wormlike aggregates are occasionally observed, alone or together with rare fibrils (Figure S2). Overall, the collected images indicate that when the AWI is removed from the samples, only few mature amyloid fibrils and/or oligomers with little, if any, capability to bind to the ThT dye can form.

This finding is further corroborated by a quantification of the amount of soluble monomeric α-Syn recovered at the end of the kinetics, through size-exclusion chromatography (SEC) analysis of aliquots of samples incubated with and without the AWI, after removal of large aggregates by centrifugation (Table 1). A comparison between the area values of the monomer peak of the injected samples versus those of samples of freshly dissolved monomeric α-Syn at concentrations ranging from 100 to 900 μM, allowed estimating the fraction of soluble α-Syn at the end of incubation in the presence/absence of the AWI. While in the presence of the AWI, ca. 40−80% of the starting amount of protein aggregated; no significant protein loss is observed in analogous samples incubated without the AWI (Table 1).

dx.doi.org/10.1021/ja412105t | J. Am. Chem. Soc. 2014, 136, 2866−2875

Table 1. Amount of Soluble α-Syn Recovered at the End of Incubation With and Without the AWI

$[\alpha\text{-Syn}]_{total}$ (μM)	AWI	[seed] (μM)	$[\alpha\text{-Syn}]_{soluble}$ (μM)	FS[a]
300	+	–	127 ± 62	0.42 ± 0.21
300	–	–	290 ± 58	0.97 ± 0.19
900	+	–	66 ± 23	0.07 ± 0.03
900	–	–	791 ± 170	0.88 ± 0.19
300	+	0.003	48 ± 32	0.16 ± 0.10
300	+	0.03	16 ± 13	0.05 ± 0.04
300	+	0.3	7 ± 17	0.02 ± 0.06
300	+	1.5	4.5 ± 2.5	0.015 ± 0.008
300	+	3	NA[b]	NA[b]
300	+	15	NA[b]	NA[b]
300	–	0.003	285 ± 50	0.95 ± 0.17
300	–	0.03	263 ± 35	0.88 ± 0.11
300	–	0.3	241 ± 35	0.80 ± 0.12
300	–	3	47 ± 32	0.16 ± 0.10
300	–	15	NA[b]	NA[b]

[a]FS refers to the fraction of soluble α-Syn in the samples and is given by the ratio between $[\alpha\text{-Syn}]_{soluble}$ and $[\alpha\text{-Syn}]_{total}$. [b]Data are not available (NA) for these samples because the amount of material in the soluble fraction is too low to result in a clear peak in the SEC profile.

Additional control experiments further confirmed that, under these experimental conditions and in the absence of the AWI, most of the protein remains in its monomeric form and that the results reported above are not affected by a potential preferential interaction of ThT with the AWI (Supplementary Results and Figure S3).

In studies with IAPP and Aβ peptides, a certain extent of aggregate formation in the absence of the AWI was observed when the concentration of the sample increased, indicating that at higher concentration these two peptides could also aggregate in the bulk, although the amount of aggregates remained lower than that obtained in analogous samples having the AWI.[24−26] To test whether similar observations apply to the case of α-Syn, kinetics at increasing concentrations (from 200 to 900 μM) of monomeric α-Syn were measured in multiple independent plates (Figure 2A). When the half-time (t_{50}) of fibril growth obtained by curve fitting of the kinetics with equation 1 (see Experimental Section) was plotted against the initial α-Syn concentration on a log−log plot, a constant decrease was observed as expected for nucleated polymerization kinetics[5,7] (Figure 2B). The intensity of ThT fluorescence at equilibrium ($FI_{485\ nm}^{eq}$) also obtained from the fitting increased linearly with the initial α-Syn concentration up to 500 μM and flattened at higher concentrations, most likely due to the higher tendency of these concentrated samples to form a gel during the measurement (Figure 2C and data not shown). Finally, SEC analysis showed that the amount of soluble protein recovered from these samples decreases as a reciprocal function of the starting protein concentration (Figure 2C). In conclusion, up to 500 μM α-Syn, a linear relation exists between the amount of aggregated protein and the ThT signal emitted at plateau.

However, despite the substantial acceleration of α-Syn aggregation kinetics at increasing concentration observed with the AWI, when such interface is removed, aggregation does not occur even at a protein concentration as high as 900 μM, as indicated by the lack of a significant increase in ThT emission over time and by the low extent of conversion of monomeric α-Syn into aggregates (Figure 2D and Table 1). These data

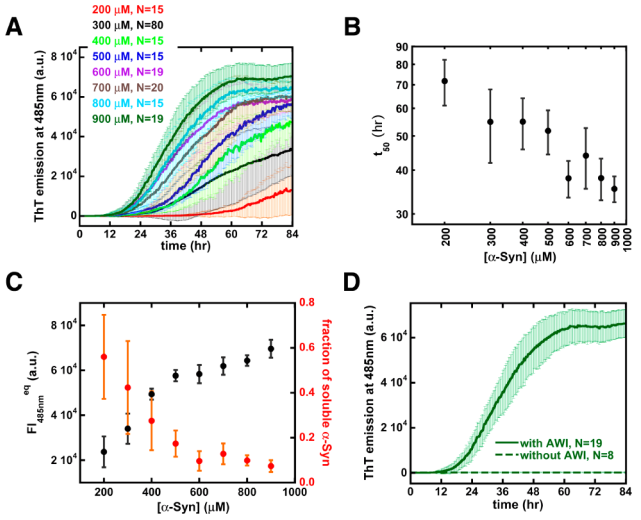

Figure 2. Concentration dependence of α-Syn aggregation with the AWI and effect of AWI removal at high α-Syn concentration. (A) ThT emission curves from samples at different α-Syn concentrations aggregated in the presence of the AWI. In all cases, a 15:1 protein/dye molar ratio was maintained. (B) Dependence of the half-time (t_{50}) of fiber growth on the concentration of α-Syn. (C) Dependence of the fluorescence intensity of ThT at equilibrium ($FI_{485\ nm}^{eq}$) (black) and of the fraction of soluble α-Syn measured by SEC (red) on the concentration of α-Syn. (D) ThT emission curves at 900 μM α-Syn concentration from wells incubated with (solid) and without (dashed) the AWI. The values of t_{50} and $FI_{485\ nm}^{eq}$ were obtained from sigmoidal fitting of the kinetics in (A) with eq 1. In all panels, error bars show the standard deviations of the averaged data sets.

suggest that, when the AWI is removed, the formation of aggregation-competent nuclei from the monomeric protein cannot occur during the monitored time scale, resulting in an inhibition of the fibrillation process. It is therefore possible to conclude that, under the investigated conditions, interfacial effects are the primary triggers of α-Syn aggregation as suggested before.[31]

Surface Activity of α-Syn Fibrils. The presented data indicate albeit indirectly that monomeric α-Syn is surface active, which is further confirmed by recently reported adsorption measurements of the protein to the AWI.[33,34] An additional question is whether the fibrils formed in the presence of the AWI may also grow at the interface and remain adsorbed to it. To investigate this aspect, atomic force microscopy (AFM) images of samples at 300 μM concentration after 4 days of incubation with the AWI were acquired. Aliquots of the samples were taken at the AWI and in the bulk. The interfacial layer was collected by a modified Langmuir−Schaefer method that ensures minimal interference from the bulk.[35] Afterward, an aliquot of the bulk of the same sample was collected, by gently inserting a needle from the bottom of the plate. The acquired images show that while at the interfacial layer a crowded network of fibrils is observed, only a few fibrils are found in the bulk fraction of these samples (Figure 3). Moreover, the fibrils taken at the AWI are embedded in a thick gel-type layer with a thickness of ca. 10−12 nm in the dried state (Figure S4).

In a control experiment, a poly(methyl methacrylate) (PMMA) cap used to remove the AWI from the same type of sample was scanned by AFM and fibrils were also observed at the PMMA−water interface (Figure S5). This result contradicts previous observation that PMMA is an inert surface

dx.doi.org/10.1021/ja412105t | J. Am. Chem. Soc. 2014, 136, 2866−2875

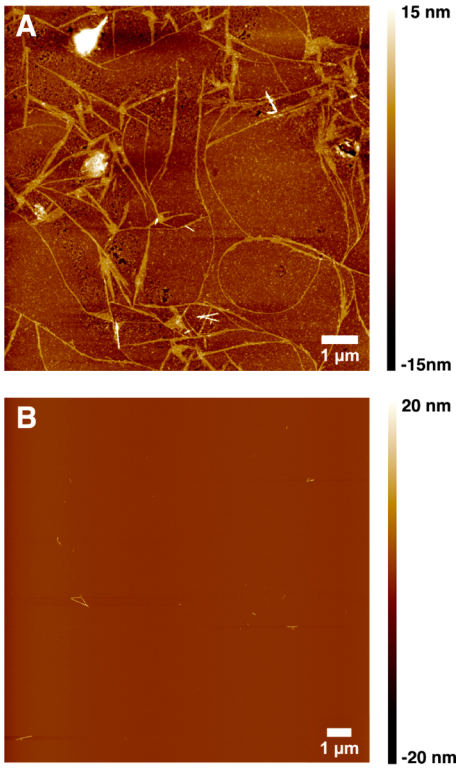

Figure 3. α-Syn fibril growth and accumulation at the AWI. (A, B) AFM images of the interfacial fibril layer (A) and of the bulk (B) fractions of a sample of 300 μM monomeric α-Syn aggregated for 4 days in the presence of the AWI.

for α-Syn aggregation to occur.[31] However, the total amount of aggregates found at the PMMA–water interface is much lower than that at the AWI, since (i) they do not lead to a significant increase in ThT emission and (ii) SEC analysis shows that most of the protein incubated without the AWI remains in its monomeric form. It is therefore possible to conclude that, in our experiments, fibril formation can occur only to a minor extent in the absence of the AWI and it appears to be limited to the PMMA surface. In the presence of the AWI instead, more protein is converted into fibrils and these are surface active, with limited desorption from the interface. The obtained data stress further the importance of interfaces in α-Syn aggregation since it is clear that no aggregation can happen in the bulk from the monomeric protein alone, over the monitored time-scale. Instead aggregation can happen only at an interface, to an extent that depends on its nature and type, with the AWI being a much stronger promoter of α-Syn aggregation with respect to the PMMA-water interface.

Effect of AWI Removal in Seeded Experiments. Seeds are often used to simplify aggregation kinetics by bypassing the rate-limiting step of the process: stochastic nucleation. Addition of seeds accelerates the process and increases its extent of reproducibility.[5,30,36] Since the formation of α-Syn fibrils from the monomeric protein can occur massively only in the presence of the AWI, it becomes interesting to study the effect of such an interface on kinetics where the growth of seeds into fibrils is monitored. To pursue this study, the aggregation of α-Syn in the presence of various amounts of seeds was monitored with and without the AWI.

A protocol to reproducibly obtain a monodisperse population of seeds in terms of its size distribution was established, by testing the sonication conditions listed in Table S1 on aged α-Syn fibrils (Supplementary Experimental Section). Figure S6A shows the average of the intensity versus size distributions measured by dynamic light scattering (DLS) and obtained by CONTIN analysis[37] of the autocorrelation functions of sixteen different preparations with the sonication protocol 8 from Table S1. The seeds used in this work appear as a single peak with an average size of 72.7 ± 13.3 nm. A representative EM picture of these seeds confirmed their rod-like morphology, with a diameter of 10–20 nm (Figure S6B). Moreover, SEC analysis indicated that little if any monomeric protein is present in these preparations (data not shown).

Such seeds were initially used in aggregation kinetics of α-Syn at fixed monomer concentration (300 μM), in the presence of the AWI. Figure 4A shows that, as expected, when the

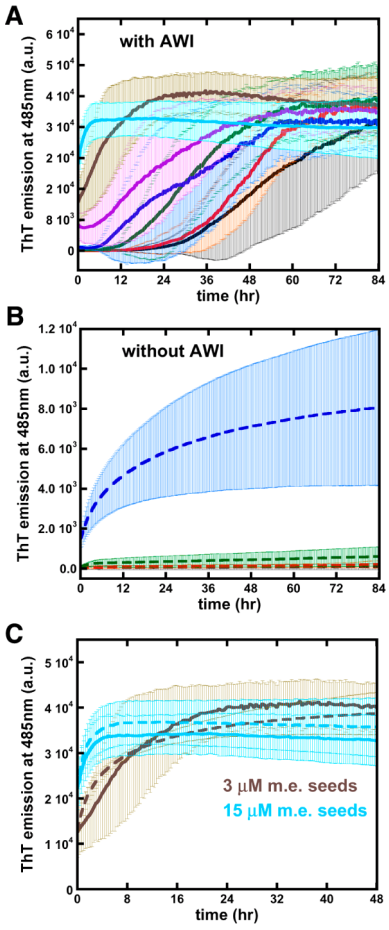

Figure 4. Effect of AWI removal on seeded aggregation kinetics. (A) ThT kinetics at 300 μM α-Syn, with the AWI and seed concentrations of 0 (black), 0.003 (red), 0.03 (green), 0.3 (blue), 1.5 (purple), 3 (brown), and 15 (light blue) μM in monomer equivalent (m.e.) units. (B) ThT kinetics without the AWI at seed concentrations from 0 to 0.3 μM (m.e.). Colors are as in panel (A). (C) ThT kinetics at 3 and 15 μM m.e. seeds with (solid) and without (dashed) the AWI. In all panels, error bars correspond to the standard deviations of the data.

concentration of seeds varies from 3 nM to 15 μM in monomer equivalent (m.e.) units, the aggregation process under the experimental conditions used for Figure 1 is substantially accelerated, until a lag-phase is not observed anymore (above 1.5 μM m.e.). Error bars report the standard deviation of data from independent experiments, each with fresh preparations of

dx.doi.org/10.1021/ja412105t | J. Am. Chem. Soc. 2014, 136, 2866–2875

seeds and monomeric protein as listed in Table S2. There is a high extent of variability in the measured kinetics. As expected however, the width of the error bars decreases with an increase in the concentration of seeds. In general, the extent of reproducibility among replicates within the same plate substantially improved at an amount of seeds corresponding to 1.5 μM m.e. (i.e., when the duration of the lag-phase started to become negligible); however, there is still variability among data obtained from different plates.

Table 1 reports the amount of soluble protein recovered from these samples, determined by SEC. When seeds are added to the samples, more α-Syn is sequestered into the aggregates, until it is not possible to detect a significant amount of soluble protein (above 1.5 μM m.e.). However, the intensity of ThT emission at plateau remains similar to that of the samples incubated without any seed or even decreases slightly (Figure 4A). The lack of correlation between emission intensity and amount of aggregated protein might be due to the higher tendency of the samples to gel, especially at high seed concentration (data not shown). Alternatively or in addition to that, more fibrils but shorter in length may form at high seed concentrations.

When the effect of AWI removal on analogous samples was tested the kinetics appeared to be dependent on the amount of added seeds (Figure 4B and C). At seed concentrations lower than 0.3 μM m.e. a nonsignificant increase in ThT emission is observed, as opposed to the *ca.* 2-fold shortening of lag-phase observed in presence of the AWI. At 0.3 μM m.e. seeds, an exponential increase in ThT emission over time is clearly observed but the fluorescence intensity at plateau is still ca. 4-fold smaller than that of corresponding samples aggregated with the AWI (Figure 4A and B). Finally, when the seed concentration reaches or becomes higher than 3 μM, the kinetics is still exponential but the plateau value becomes similar to that obtained in the presence of the AWI (Figure 4C). The fact that under these conditions the samples without AWI also aggregate is additionally confirmed by EM analysis and by the fact that the samples are gelatinous (Figure S7 and data not shown). The morphology of the fibrils is similar to the one from conditions with the AWI. Moreover, SEC analysis revealed that most of the initial amount of protein is now converted into aggregates (Table 1). However, at equal seed concentration, the extent of monomer conversion into aggregates in the absence of the interface is, if detectable, always lower than that obtained with the AWI.

An intriguing observation emerging from the kinetics in Figure 4 is that when aggregation occurs without the AWI, it proceeds faster than with the AWI and it does not show any lag-phase, while kinetics measured with the AWI still do. For example, despite the plateau value being smaller, the increase in ThT emission measured at 0.3 μM m.e. seeds without the AWI is faster than the corresponding one with the AWI, which still shows a lag-phase (Figure 4A and B). A difference in overall aggregation rate with and without the AWI is observed also at 3 μM and 15 μM m.e. seed concentrations (Figure 4C). To investigate this aspect further, a kinetic experiment was then performed at 37 °C on a shorter time-scale (21 h), under completely quiescent conditions and collecting data every 5 min, to better resolve the early phase of aggregation. In seeded experiments, the early phase of the kinetics should reflect mainly the contribution of seeds elongation to the overall process, while nucleation events of either primary (depending only on the monomer) or secondary (depending only on the aggregates or on both the monomer and the aggregates) nature become dominant at longer times.[5,38]

Figure 5 shows the result of such an experiment. In the absence of the AWI, aggregation kinetics are exponential at

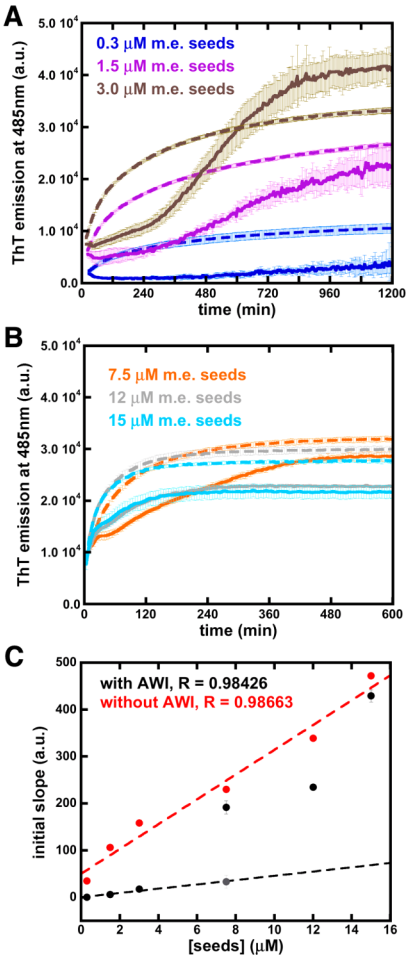

Figure 5. Effect of AWI removal on the early phase of seeded kinetics. (A, B) ThT kinetics at 300 μM α-Syn, 20 μM ThT and seeds from 0.3 to 3.0 μM (A) and from 7.5 to 15 μM m.e. (B). Solid and dashed curves refer to the results with and without the AWI, respectively; error bars to their standard deviation. (C) Dependence of the initial slope of the measured kinetics on the concentration of seeds. Black and red data points refer to the data with and without the AWI, respectively. The gray data point at 7.5 μM m.e. seeds corresponds to the slope of the kinetic data measured with the AWI from 30 to 50 min. The dashed lines in figure were obtained by linear fitting of the data representing the initial slope measured with (black) and without (red) the AWI. In the first case, only the data points reporting on interfacial aggregation were fitted.

every seed concentration used, indicating that, rather than the formation of new aggregates, it is the elongation of the preadded seeds that is measured under these conditions. In the presence of the interface instead the formation of new aggregates still contributes to the measured kinetics. Indeed, at seed concentrations from 0.3 to 3 μM m.e., the kinetics are progressively accelerated, but still sigmoidal in shape (Figure 5A). At 7.5 μM m.e. seed concentration, the kinetics has an initial slope similar to that measured without the AWI but it is subsequently delayed (between ca. 30−50 min), having still some extent of cooperativity (Figure 5B). A possible interpretation might be that, at this concentration of seeds,

dx.doi.org/10.1021/ja412105t | J. Am. Chem. Soc. 2014, 136, 2866−2875

aggregation could rapidly start in the bulk and be subsequently slowed when the seeds themselves also become adsorbed to the AWI. Only at the highest seed concentrations the kinetics become more exponential-like in shape, but they are still delayed. To isolate the elongation contribution from others and investigate how it depends on the amount of seeds, both at the interface and in the bulk, a linear regression of the data measured in the very early phase of the kinetics[38] was performed (Figure 5C). In the case of the kinetics with the AWI and seed concentrations between 0.3 and 3.0 μM m.e., the data collected during the first 50 min were not included in the fitting as the ThT signal slightly decreased during this time. This effect has been observed also in another study where the fluorescence was collected from the bottom of the plate and was attributed to an interaction between the dye and the surface of the plate.[25] However, since it is observed only in the presence of the AWI and at low seed concentrations, it may also be due to adsorption of the seeds to the AWI. At 7.5 μM m.e. seeds, linear fitting was performed first with the data up to 30 min and then with those between 30 and 50 min, to discriminate between bulk and interfacial contributions, respectively. Overall, the results show that, both with and without the AWI, the slope varies linearly with the concentration of seeds, even if in the first case fewer conditions could be evaluated without interference from the bulk. Such linear scaling of the initial slope has been predicted to occur at the early times of seeded kinetics at fixed monomer concentration, under conditions where the contribution of primary nucleation can be neglected.[38] Moreover, the data indicate that at fixed seed concentration the initial slope in the absence of the AWI is up to one order of magnitude higher than the one measured with the AWI.

The samples recovered at the end of this shorter experiment were also analyzed by SEC and, similarly to the case of the longer kinetics, the amount of α-Syn remaining in solution, when detectable, was always slightly lower in the presence of the AWI, despite the ThT plateau values being similar or even lower than those obtained without the AWI (data not shown). This indicates that, when the AWI is present, more protein is converted into aggregates in presence of seeds, even if the overall process is slower than in the absence of the AWI. Thus, more aggregates are created in presence of the AWI as it enables de novo nucleation events (either primary or secondary) to occur, leading to the formation of new seed-competent aggregates that contribute to the kinetics.

DISCUSSION

Role of Interfaces in the Aggregation of Monomeric α-Syn. Although HHIs are constantly present in aggregation kinetic experiments performed in vitro, their influence on the process is still poorly understood and mostly neglected. In this work, the effect of the AWI on α-Syn aggregation was studied by replacing it with a PMMA−water interface. Compared to previous similar setups,[25,26] ours was optimized to ensure a better sealing on longer duration experiments (Supplementary Results and Figure S1). Removal of the AWI has dramatic consequences on α-Syn aggregation as monitored by time-resolved ThT fluorescence and complementary methods such as SEC, EM, pentamer formyl thiophene acetic acid (p-FTAA) binding measurements and DLS (Figures 1 and 2, Table 1, Figures S2 and S3). Monomeric α-Syn at concentrations up to 900 μM does not aggregate without the AWI being present (Figures 1 and 2). Instead, analogous samples incubated with the AWI clearly form amyloid fibrils (Figures 1 and 2, Table 1). The variability in our experiments with the AWI can be attributed to the stochastic nature of nucleated-polymerization processes, which influences aggregation kinetics most prominently in experiments without extensive shaking. Moreover, the poor degree of reproducibility of α-Syn aggregation kinetics at neutral pH is well documented and was observed before even in agitated experiments.[30] Overall, our data strengthen the notion that a catalytic-like interface is critical for α-Syn aggregation to occur[31] as, in respect to this previous work, here a concentration more than 10 times higher is used, but still no aggregation is detected in absence of the AWI interface.

However, despite the lack of a significant increase in ThT emission and the fact that most of the protein remains in its monomeric form when the AWI is removed, the PMMA surface is not fully inert as observed before,[31] since some fibrils were detected by AFM at the cap surface (Figure S5). This is in line with the fact that even if an increase in ThT fluorescence was initially not observed in sealed (without AWI) α-Syn samples incubated in the presence of hydrophilic glass beads,[31] more sensitive techniques such as three-dimensional super-critical angle fluorescence (3D-SAF) microscopy recently revealed that this protein can aggregate to some extent even on such hydrophilic surface.[39] In addition, the air−water and PMMA−water interfaces differ not only in their hydrophobicity, but also in their nature: the former being a gas−liquid interface; the latter a solid−liquid interface. The α-Syn chains adsorbed at the AWI may remain highly dynamic, favoring protein−protein interactions and interfacial diffusion. Instead, the α-Syn molecules adsorbed at the PMMA cap may undergo local aggregation but not be able to diffuse because of the rigidity of such solid surface. It is therefore likely that a higher mobility of the adsorbed protein at the AWI as compared to the PMMA−water interface will further promote its aggregation, as recently observed in the case of Aβ.[40] Taken together, the data presented here clearly show that the AWI is a much stronger promoter of aggregation than the PMMA−water interface and that ThT binding kinetics in presence of the PMMA-water interface can provide insights on the effect of AWI removal.

Multiple hypotheses have been formulated so far to explain the role of the AWI, and more generally of HHIs, in amyloid formation. HHIs can for example promote aggregation by spatially concentrating surface-active proteins and peptides and increasing their rate of collision.[25] This would lead to an increase in the effective concentration of the macromolecule at the interface with respect to the bulk, which would in turn result in nucleation occurring preferentially at the interface.[24−26] Adsorption of a protein to the interface can also promote structural changes and a spatial alignment of the polypeptide chain, which can influence aggregation.[17] The IAPP peptide has been observed to adsorb to the AWI as well as to a phospholipid monolayer, and to adopt in both cases an α-helical conformation followed by subsequent transition over time to a β-sheet-rich structure, with the β-sheets lying parallel to the interface.[21] A recent study on three different model peptides able to form both α-helical and β-sheet-rich structures revealed that even at high (up to the order of mM) local peptide concentration, the AWI can lead to the formation of a stable α-helical state, depending on the peptide.[22] However, when the extent of conformational order at the interface becomes high enough to induce the α-helical states to align in a parallel fashion, all peptides convert into a β-sheet-rich

dx.doi.org/10.1021/ja412105t | J. Am. Chem. Soc. 2014, 136, 2866−2875

structure.[22] These data indicate that interfaces may play pluripotent roles in the aggregation kinetics of amyloidogenic peptides/proteins, and in particular in the formation of an aggregation-competent nucleus, by increasing the local concentration as well as ordering and possibly aligning the peptides/proteins. In the case of liquid−liquid or gas−liquid interfaces, these processes are facilitated by in-plane diffusion, whereas for a liquid−solid interface diffusion rates are highly reduced, independent of the exact interfacial energy present.

It is intriguing to speculate whether α-Syn may behave similarly to the aforementioned peptides. α-Syn is an intrinsically disordered protein but its sequence contains seven 11-mer repeats that form an amphipathic α-helix in the presence of lipid vesicles comprising negatively charged phospholipids.[41,42] Furthermore, α-Syn has been recently observed to adopt an α-helical conformation at the AWI.[33] It is therefore likely that the 11-mer repeats in the α-Syn sequence are responsible for the surface activity of this protein and undergo a change in conformation toward an α-helix-rich state at the AWI. However, no spontaneous transition toward a β-sheet-rich structure was observed at the AWI, at least over the monitored time-scale and at the investigated concentration,[33] while in our study the aggregation of α-Syn into amyloid fibrils and thus a β-sheet-rich state at the AWI is documented. Based on these observations we propose that a critical balance between interface-mediated aggregation into fibrils and interface-induced stabilization of an α-helical state may exist. Depending on the extent of α-Syn accumulation at the interface and degree of interfacial order, the stability of the α-helical state could vary and this may explain why controversial results are often reported on the role of lipids and membranes in the aggregation of this protein.[39,43,44]

Seeded Aggregation of α-Syn in the Absence of the AWI. To elucidate whether the AWI plays its role during the nucleus formation process or the fibril elongation process or both, aggregation kinetics in presence/absence of the AWI were measured upon addition of increasing amounts of seeds (Figures 4 and 5). As shown in Figure 4B, in the absence of the AWI, no aggregation is observed at seed concentrations lower than 0.03 μM m.e., either because of the lack of a substantial amount of active seeds in the sample or because the experimental sensitivity and the duration of the experiment were not enough to detect a significant increase in amyloid growth. At higher seed concentrations (from 0.03 μM upward), amyloid aggregation occurs, either partially or fully, at least in terms of intensity of ThT emission at equilibrium. The kinetics is exponential, indicating a first order reaction. Furthermore, when the early times of such kinetics are investigated in more detail in a fully quiescent experiment, the initial slope is found to linearly increase with the amount of seeds (Figure 5C). These data are in line with models of aggregation kinetics in absence of any nucleation event.[36] Nucleation pathways are generally defined as primary if the newly formed aggregates originate from the soluble protein only, secondary if existing aggregates are also involved in the formation of new ones.[5,7] Examples of secondary nucleation pathways are fibril fragmentation, amyloid surface-catalyzed nucleation and fibril branching.[5,7,38] Since aggregation in the bulk occurs only when seeds are added, primary nucleation cannot take place in the bulk (Figures 1 and 2). Interestingly, as first-order-like kinetics are obtained without the AWI, secondary nucleation pathways are also not taking place in the bulk. The kinetics in Figure 5 were measured under quiescent conditions so fibrils fragmentation may indeed not contribute much here, but other secondary nucleation pathways such as amyloid surface-catalyzed nucleation and fibrils branching appear also not to contribute to the presented bulk measurements.

Seeded Aggregation of α-Syn in the Presence of the AWI. In contrast to the simple, first-order-like, seeded aggregation kinetics measured in absence of the AWI, the seeded aggregation behavior of α-Syn in presence of the AWI appears to be more complex. In 4-days-long experiments, the kinetics measured with the AWI up to 1.5 μM m.e. seed concentration are accelerated with respect to those obtained without seeds, but they still show an inflection point at which the rate of the reaction increases and the overall curve is sigmoidal (Figure 4A). This observation suggests that, in parallel to elongation of the added seeds, a nucleation-dependent pathway is present. Moreover, the existence of the inflection point indicates that the elongation of the added seeds is less effective than the nucleation-dependent pathway.[36,38] Since it is unlikely that primary nucleation alone could be responsible for this dominating effect because it occurs on a longer time scale (at least twice longer), as judged by the kinetics in the absence of seeds, the observed dominant nucleation-dependent process is proposed to be a secondary pathway. Similar considerations apply to the 1-day-long experiments in Figure 5. Further support to a secondary nucleation process being active here is the finding that although the initial slope of seeded aggregation kinetics in presence of the AWI is one order of magnitude slower than the one in the absence of the AWI, much less seeds are necessary to accelerate aggregation in presence of the AWI (Figures 4 and 5C). This explains also why SEC analysis shows that in the presence of the AWI more protein is converted into aggregates, even if the process is slower; that is, it is most likely due to the proliferation in the number of aggregates observed only when the AWI is present (Table 1). As these experiments are mostly or even fully quiescent, it is unlikely that the major secondary nucleation pathway involved in our seeded kinetics is fragmentation. Surface-catalyzed nucleation and branching could instead be the active secondary pathways at the AWI. Support to this hypothesis is also based on the fact that the AFM images of the aggregates at the interface in Figures 3 and S4 indicate that many short amyloid fibrils are associated and/or originating from longer ones. At increasing amounts of seeds the kinetics becomes more exponential-like but it is still delayed. This could be due to the effect of the adsorption of the seeds themselves to the AWI, which results in slower growth.

While preparing this paper, a study of seeded kinetics of IAPP with and without the AWI was published.[45] However, our results do not fit with their conclusions on the role of the AWI in seeded kinetics as the intensity of ThT emission at plateau does not reflect the extent of aggregation of the sample. Rather, our SEC analysis shows that, at least in the case of α-Syn, a higher conversion of monomeric protein into aggregates is always found in the samples incubated with the AWI. However, an interesting aspect, even if not discussed, of their results is that the seeded kinetics of IAPP without the AWI also appear to be more concave in shape than those measured with the AWI.[45]

Overall, the kinetics reported here with and without seeds indicate that no nucleation event, either primary or secondary, takes place in the bulk, at least under the conditions tested, and that only in the presence of the interface nucleation pathways of both types (primary and secondary) occur and even become

dominant over the elongation of preformed seeds. The nature of the secondary nucleation pathway is proposed to be either amyloid surface-catalyzed nucleation or branching. In Figure 6, these concepts are summarized in a schematic fashion.

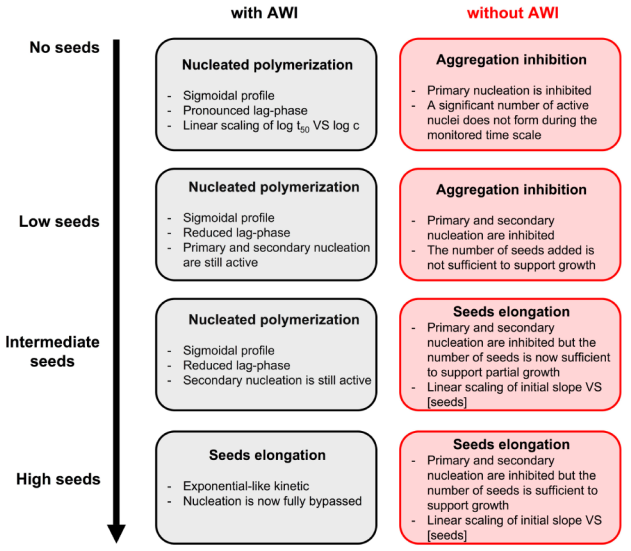

Figure 6. Schematic explanation of the obtained results. In this figure, the results of the kinetic data measured in the presence (gray-shaded boxes) and absence (red-shaded boxes) of the AWI at different amounts of seeds are summarized and interpreted. The arrow on the left side indicates the increase in seed concentration.

CONCLUSION

The study of α-Syn aggregation into amyloid fibrils presented here demonstrates the importance of interfaces (here the AWI) for aggregation to occur both in presence and absence of seeds. While the AWI is crucial for the formation of seed-competent nuclei, nuclei are not formed in the bulk. When nuclei are added to the sample, their elongation process is faster in the bulk, while at the AWI it is attenuated at least by one order of magnitude. Finally, a secondary nucleation pathway (probably surface-catalyzed nucleation) appears to be prominent at the AWI, while it is absent in the experiments with the solid–liquid PMMA–water interface, where interfacial diffusion is highly reduced. These findings indicate that the aggregation process of α-Syn in vitro is complex, depending, in addition to the solution conditions and protein concentration, also on the presence and the properties of an interface and on the interplay between the bulk and this interface. Obviously, the complexity of this aggregation process may increase further in vivo as many different buffer regimes, membranes, compartments, chaperones, and so forth are present in a cellular environment. The presented results help to interpret part of this complexity and may become even more important when considering that recent evidence on the spreading of Parkinson's disease and other synucleinopathies suggests that the diffusion of the aggregates in the body is mediated by the cell-to-cell transmissibility of α-Syn fibrils that act as seeds and induce the aggregation of the soluble protein in the host cell.[28]

EXPERIMENTAL SECTION

Thioflavin T (ThT) Binding Kinetics with and without AWI in 96-Well Plates. ThT dye from Sigma-Aldrich (St. Louis, MO) was dissolved in PBS + 0.05% (w/v) NaN_3, filtered with a 0.2 μm filter, and its concentration was then determined by ultraviolet–visible (UV–vis) absorbance ($\varepsilon_{412\ nm}$ = 36 000 M^{-1} cm^{-1}). Stocks at 1 mM concentration were prepared and stored at −20 °C until use. Aliquots of monomeric α-Syn, ThT, and seeds (when necessary) were diluted at the desired final concentration with degassed PBS + 0.05% (w/v) NaN_3 in dark glass vials. A 15:1 monomeric protein/dye molar ratio was used in all experiments. The samples were then incubated in an oven at 55 °C for 10 min before being distributed into the wells of the plate. Non-binding, clear bottom, black 96-well plates (cat. no. 655906 from Greiner Bio-One, Stonehouse, U.K.) were used. Functional groups similar to those of polyethylene glycol are used to make the polystyrene plastic hydrophilic (personal information from Greiner Bio-One). Details on how wells with and without the AWI are prepared are in the Supporting Information. Control wells with ThT alone or with the appropriate amount of seeds were also prepared. The plate was then covered with an AMPLIseal transparent adhesive from Greiner Bio-One. All caps and glass vials were cleaned with 5% (v/v) Deconex 11 (Applichem, Darmstadt, Germany), rinsed with Milli-Q water, and reused. Although this procedure did not completely remove the fibrils at the level of the cap as judged by AFM imaging, these residual fibrils did not lead to significant changes in ThT intensity at time zero and to the formation of aggregates in the bulk.

Fluorescence measurements were performed with an Enspire 2300 Multilabel Reader (PerkinElmer, Turku, Finland). The temperature was set to 37 and 41 °C for the lower and upper heaters, respectively, to prevent condensation. The intensity of ThT emission at 485 nm was collected every 20 min in bottom excitation/emission mode at a fixed focal height of 3 mm (close to the bottom of the well). The heights of the AWI and the PMMA-water interfaces are similar. These measurements are therefore bulk measurements, but when a large amount of aggregates form at the AWI, they also report on the contribution of the interface to the signal, similarly to what as been observed by others.[25,26] Excitation was at 450 nm, with 10 flashes. The signal was collected at 5 different spots on the XY-plane and averaged.

In 4-days-long kinetics, data were collected every 20 min and before each measurement the plate was shaken for 5 s at 500 rpm in orbital mode. In 21-h-long kinetics the plate was left quiescent and data were collected every 5 min. The samples for the shorter kinetics were prepared immediately before being dispensed into the plate, without undergoing incubation in the oven. Signals from control wells were subtracted to those of the samples. The half-time (t_{50}) of fiber growth and the fluorescence intensity of ThT at equilibrium ($FI_{485\ nm}^{eq}$) were obtained by fitting the sigmoidal curves measured at increasing α-Syn concentration and in the presence of the AWI using the following equation:

$$FI_{485nm}(t) = \frac{FI_{485nm}^{eq}}{1 + e^{-(t-t_{50})/\tau}} \quad (1)$$

where $1/\tau$ is the apparent rate constant for fibril growth.[13,46] A linear regression of the data at early times recorded in 21-h-long seeded kinetics in the presence/absence of the AWI was performed as described, to obtain the initial slope.[38]

Electron Microscopy (EM). Aliquots of 4 μL of seeds or of samples collected at the end of a plate reader assay were deposited on a carbon coated copper grid (Electron Microscopy Sciences, Hatfield, PA) for 30 s and excess sample was removed with filter paper. The surface of the grid was then washed three times with Milli-Q water and stained with 2% uranyl acetate for 10 s. The samples were then imaged with a FEI Morgagni TEM electron microscope (FEI, Hillsboro, OR) operating at 100 kV.

Size-Exclusion Chromatography (SEC). Aliquots of 50 μL of samples collected at the end of a plate reader assay were injected into a TSKgel G4000PWxl SEC column (Tosoh Bioscience, Tokyo, Japan), after removal of large aggregates by centrifugation at 20 psi (ca. 120 000g) for 30 min in an Airfuge (Beckman Coulter, Brea, CA). The column was connected to a 1200 Series chromatographic system from Agilent Technologies (Santa Clara, CA) and equilibrated in 50 mM phosphate buffer, pH 6.5, with 150 mM sodium chloride and 0.05% (w/v) NaN_3. The elution profile at 0.5 mL/min was obtained by

dx.doi.org/10.1021/ja412105t | J. Am. Chem. Soc. 2014, 136, 2866–2875

monitoring the absorbance signal at 280 nm and the eluting peaks were integrated with the Chemstation software.

Atomic Force Microscopy (AFM) images. The fibril/protein layer at the AWI was transferred onto freshly cleaved mica using a modified Langmuir–Schaefer technique.[35] As the diameter of the wells in the 96-well plate used is smaller than the standard size of mica sheets, mica discs with 3 mm diameter were punched out of a larger piece. After cleavage, the mica sheet was lowered into the well and briefly brought into contact horizontally with the sample surface. Care was taken to approach the sample in the center of the well to prevent an uneven deposition due to the meniscus of the sample. A subsequent dip into ethanol allowed for the removal of nonadsorbed material and artifact-free drying of the sample.[47] Aliquots for AFM imaging of the bulk fraction were then extracted from the plate by inserting a needle through the bottom of the well of interest and removing some of the liquid at a position as far away from the upper interface as possible. A volume of 10 μL was then deposited onto a piece of freshly cleaved mica and incubated for 2 min. After rinsing with 1 mL of Milli-Q water, the sample was gently dried with an air gun. Imaging was performed on a Nanoscope VIII Multimode scanning probe microscope (Veeco Instruments, Plainview, NY) in tapping mode in air at a scan rate of 0.1 Hz.

■ ASSOCIATED CONTENT

Supporting Information

Supplementary results on the design of the experimental setup and on control experiments to confirm that AWI removal inhibits aggregation. Experimental procedures for protein purification, sample preparation, seeds preparation, p-FTAA fluorescence, and DLS. Supplementary figures and tables described in the paper. This material is available free of charge via the Internet at http://pubs.acs.org.

■ AUTHOR INFORMATION

Corresponding Author

roland.riek@phys.chem.ethz.ch

Notes

The authors declare no competing financial interest.

■ ACKNOWLEDGMENTS

The authors would like to acknowledge David Stapfer (ETH Zürich, Switzerland) for manufacturing all caps used in this work and Dr. Jozef Adamcik for his help in imaging the caps by AFM. Dr. Letitia Jean and Prof. David Vaux (University of Oxford, U.K.) are acknowledged for providing detailed information on the caps used in their studies and Dr. Peter Nilsson (Linköping University, Sweden) for providing the p-FTAA dye. Prof. Massimo Morbidelli, Dr. Paolo Arosio (University of Cambridge, U.K.), and Dr. Alois Renn (ETH Zürich, Switzerland) are also acknowledged for helpful discussions and technical support. This work was supported by the Swiss National Foundation (SNF).

■ REFERENCES

(1) Invernizzi, G.; Papaleo, E.; Sabate, R.; Ventura, S. *Int. J. Biochem. Cell Biol.* **2012**, *44*, 1541.
(2) Greenwald, J.; Riek, R. *Structure* **2010**, *18*, 1244.
(3) Chiti, F.; Dobson, C. M. *Annu. Rev. Biochem.* **2006**, *75*, 333.
(4) Eichner, T.; Radford, S. E. *Mol. Cell* **2011**, *43*, 8.
(5) Cohen, S. I.; Vendruscolo, M.; Dobson, C. M.; Knowles, T. P. *J. Mol. Biol.* **2012**, *421*, 160.
(6) Campioni, S.; Monsellier, E.; Chiti, F. In *Protein Misfolding Diseases: Current and Emerging Principles and Therapies*; Ramirez-Alvarado, M., Kelly, J. W., Dobson, C. M., Eds.; John Wiley & Sons Inc., Hoboken, NJ, 2010.
(7) Ferrone, F. *Methods Enzymol.* **1999**, *309*, 256.
(8) Wetzel, R. *Acc. Chem. Res.* **2006**, *39*, 671.
(9) Biancalana, M.; Koide, S. *Biochim. Biophys. Acta* **2010**, *1804*, 1405.
(10) LeVine, H., 3rd. *Protein Sci.* **1993**, *2*, 404.
(11) Castillo, V.; Grana-Montes, R.; Sabate, R.; Ventura, S. *Biotechnol. J.* **2011**, *6*, 674.
(12) Seeliger, J.; Estel, K.; Erwin, N.; Winter, R. *Phys. Chem. Chem. Phys.* **2013**, *15*, 8902.
(13) Nielsen, L.; Khurana, R.; Coats, A.; Krokjaer, S.; Brange, J.; Vyas, S.; Uversky, V. N.; Fink, A. L. *Biochemistry* **2001**, *40*, 6036.
(14) Sasahara, K.; Yagi, H.; Naiki, H.; Goto, Y. *J. Mol. Biol.* **2007**, *372*, 981.
(15) Sasahara, K.; Yagi, H.; Sakai, M.; Naiki, H.; Goto, Y. *Biochemistry* **2008**, *47*, 2650.
(16) Ghiem, L.; Lorenzen, N.; Otzen, D. E. *Methods* **2011**, *53*, 295.
(17) Mezzenga, R.; Fisher, P. *Rep. Prog. Phys.* **2013**, *76*, 046601.
(18) Soreghan, B.; Kosmoski, J.; Glabe, C. *J. Biol. Chem.* **1994**, *269*, 28551.
(19) West, M. W.; Wang, W.; Patterson, J.; Mancias, J. D.; Beasley, J. R.; Hecht, M. H. *Proc. Natl. Acad. Sci. U.S.A.* **1999**, *96*, 11211.
(20) Schladitz, C.; Vieira, E. P.; Hermel, H.; Möhwald, H. *Biophys. J.* **1999**, *77*, 3305.
(21) Lopes, D. H.; Meister, A.; Gohlke, A.; Hauser, A.; Blume, A.; Winter, R. *Biophys. J.* **2007**, *93*, 3132.
(22) Hoernke, M.; Falenski, J. A.; Schwieger, C.; Koksch, B.; Brezesinski, G. *Langmuir* **2011**, *27*, 14218.
(23) Morris, V. K.; Ren, Q.; Macindoe, I.; Kwan, A. H.; Byrne, N.; Sunde, M. *J. Biol. Chem.* **2011**, *286*, 15955.
(24) Morinaga, A.; Hasegawa, K.; Nomura, R.; Ookoshi, T.; Ozawa, D.; Goto, Y.; Yamada, M.; Naiki, H. *Biochim. Biophys. Acta* **2010**, *1804*, 986.
(25) Jean, L.; Lee, C. F.; Lee, C.; Shaw, M.; Vaux, D. J. *FASEB J.* **2010**, *24*, 309.
(26) Jean, L.; Lee, C. F.; Vaux, D. J. *Biophys. J.* **2012**, *102*, 1154.
(27) Hobley, L.; Ostrowski, A.; Rao, F. V.; Bromley, K. M.; Porter, M.; Prescott, A. R.; Macphee, C. E.; van Aalten, D. M.; Stanley-Wall, N. R. *Proc. Natl. Acad. Sci. U.S.A.* **2013**, *110*, 13600.
(28) Goedert, M.; Spillantini, M. G.; Del Tredici, K.; Braak, H. *Nat. Rev. Neurol.* **2013**, *9*, 13.
(29) Spillantini, M. G.; Schmidt, M. L.; Lee, V. M.; Trojanowski, J. Q.; Jakes, R.; Goedert, M. *Nature* **1997**, *388*, 839.
(30) Ghiem, L.; Otzen, D. E. *Anal. Biochem.* **2010**, *400*, 270.
(31) Pronchik, J.; He, X.; Giurleo, J. T.; Talaga, D. S. *J. Am. Chem. Soc.* **2010**, *132*, 9797.
(32) Krammer, C.; Schatzl, H. M.; Vorberg, I. *Prion* **2009**, *3*, 206.
(33) Wang, C.; Shah, N.; Thakur, G.; Zhou, F.; Leblanc, R. M. *Chem. Commun. (Cambridge, U.K.)* **2010**, *46*, 6702.
(34) Chaari, A.; Horchani, H.; Frikha, F.; Verger, R.; Gargouri, Y.; Ladjimi, M. *Int. J. Biol. Macromol.* **2013**, *58*, 190.
(35) Jordens, S.; Isa, L.; Usov, I.; Mezzenga, R. *Nat. Commun.* **2013**, *4*, 1917.
(36) Cohen, S. I.; Vendruscolo, M.; Dobson, C. M.; Knowles, T. P. *Int. J. Mol. Sci.* **2011**, *12*, 5844.
(37) Provencher, S. W. *Comput. Phys. Commun.* **1982**, *27*, 229.
(38) Lorenzen, N.; Cohen, S. I.; Nielsen, S. B.; Herling, T. W.; Christiansen, G.; Dobson, C. M.; Knowles, T. P.; Otzen, D. *Biophys. J.* **2012**, *102*, 2167.
(39) Rabe, M.; Soragni, A.; Reynolds, N. P.; Verdes, D.; Liverani, E.; Riek, R.; Seeger, S. *ACS Chem Neurosci.* **2013**, *4*, 408.
(40) Shen, L.; Adachi, T.; Vanden Bout, D.; Zhu, X. Y. *J. Am. Chem. Soc.* **2012**, *134*, 14172.
(41) Davidson, W. S.; Jonas, A.; Clayton, D. F.; George, M. *J. Biol. Chem.* **1998**, *273*, 9443.
(42) Mizuno, N.; Varkey, J.; Kegulian, N. C.; Hegde, B. G.; Cheng, N.; Langen, R.; Steven, A. C. *J. Biol. Chem.* **2012**, *287*, 29301.
(43) Zhu, M.; Fink, A. L. *J. Biol. Chem.* **2003**, *278*, 16873.
(44) Necula, M.; Chirita, C. N.; Kuret, J. *J. Biol. Chem.* **2003**, *278*, 46674.

(45) Trigg, B.; Lee, C. F.; Vaux, D. J.; Jean, L. *Biochem. J.* **2013**, *456*, 67.
(46) Jeong, J. S.; Ansaloni, A.; Mezzenga, R.; Lashuel, H. A.; Dietler, G. *J. Mol. Biol.* **2013**, *425*, 1765.
(47) Ray, M. A.; Jia, L. *Adv. Mater.* **2007**, *19*, 2020.